SUPPORTING INFORMATION

Venom peptides with dual modulatory activity on the voltage-gated sodium channel $Na_V1.1$ provide novel leads for development of anti-epileptic drugs

Chun Yuen Chow[1], Yanni K.-Y. Chin[1], Andrew A. Walker[1], Shaodong Guo[1], Linda V. Blomster[1], Micaiah J. Ward[2], Volker Herzig[1], Darin R. Rokyta[2] and Glenn F. King[1,*]

[1]Institute for Molecular Bioscience, The University of Queensland, Brisbane QLD 4072, Australia
[2]Department of Biological Science, Florida State University, Tallahassee, FL, 32306, USA

*Address for correspondence: Prof. Glenn F. King, Institute for Molecular Bioscience, The University of Queensland, Brisbane QLD 4072, Australia. Email: glenn.king@imb.uq.edu.au; Phone: +61 3346 2025.

Keywords

Voltage-gated sodium channel, Dravet syndrome, antiepileptic drug, venom peptide, electrophysiology, gating modifier toxin, protein structure

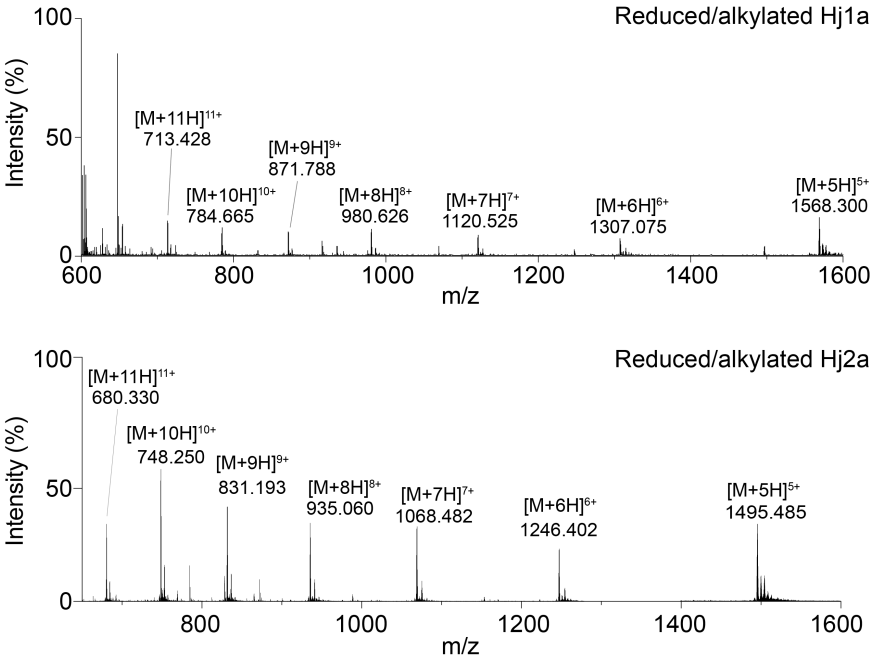

z	Observed ion (m/z)	Observed monoisotopic mass
+11	713.428	7836.6277
+10	784.665	7836.5770
+9	871.788	7837.0263
+8	980.626	7836.9496
+7	1120.525	7836.6239
+6	1307.075	7836.4062
+5	1568.300	7836.4635
		7836.6677

z	Observed ion (m/z)	Observed monoisotopic mass
+11	680.330	7472.5497
+10	748.250	7472.4270
+9	831.193	7471.6173
+8	935.060	7472.4216
+7	1068.482	7472.3229
+6	1246.402	7472.3682
+5	1495.485	7472.3885
		7472.2993

Supplementary Fig. S1 Reduction and alkylation of Hj1a and Hj2a. Mass spectra showing the monoisotopic mass of reduced/alkylated Hj1a (7,836.67 Da; top panel) and Hj2a (7,472.30 Da; bottom panel).

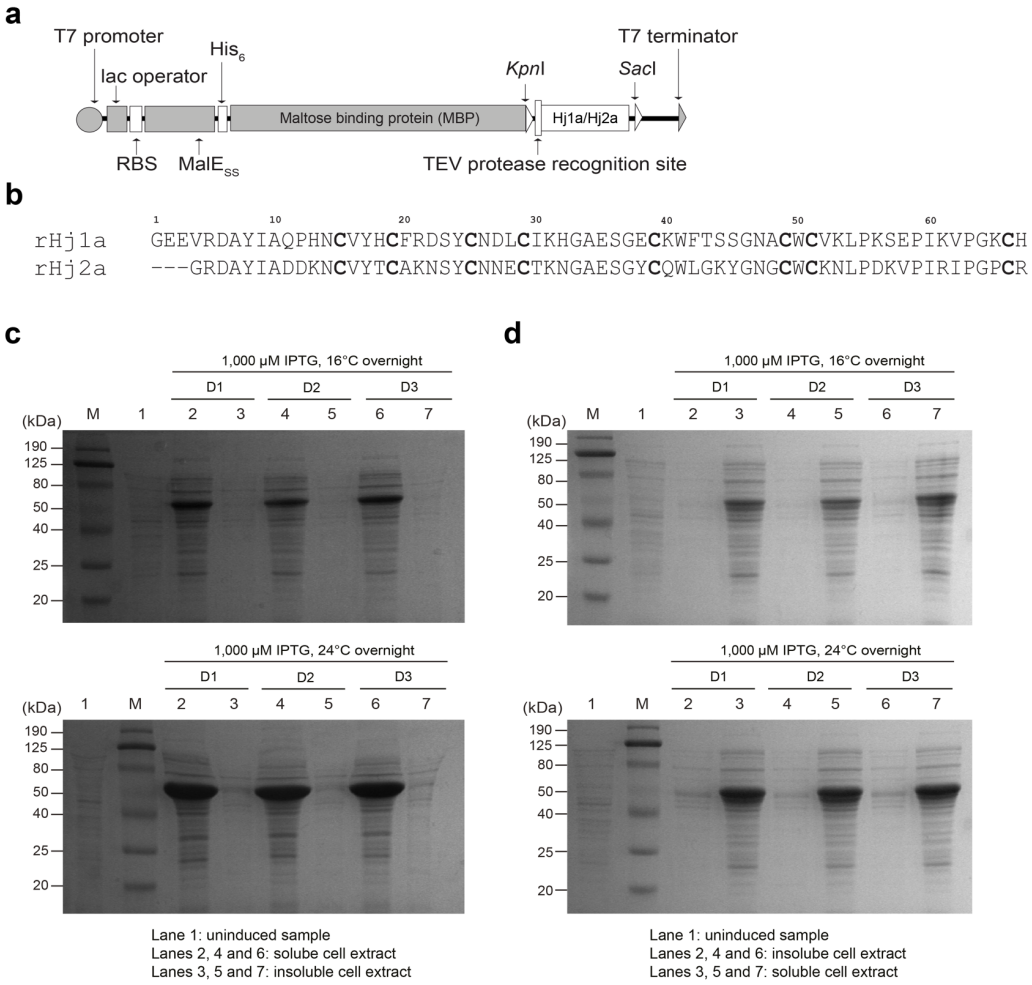

Supplementary Fig. S2 Small-scale expression of His_6-MBP-Hj1a and His_6-MBP-Hj2a. **a** Schematic representation of the pLIC vector used for periplasmic expression of rHj1a and rHj2a. The coding region includes a $MalE_{SS}$ for periplasmic export, a His_6 affinity tag, a MBP fusion tag to enhance solubility, and a codon-optimised gene encoding the peptide, with a TEV protease recognition site inserted between the MBP and toxin-coding regions. The locations of key elements of the vector are shown, including the ribosome-binding site (RBS). **b** A non-native N-terminal Gly residue was added to the Hj1a coding sequence to optimise fusion protein cleavage as the native N-terminal residue (Glu) is a non-preferred residue for the P1' site of TEV protease. Cys residues are highlighted in bold. **c** Coomassie-stained SDS-PAGE gel analysis of the small-scale expression of rHj1a in *E. coli* strain BL21. Three colonies were selected and labelled D1, D2 and D3. Expression of the fusion protein was induced with 1 mM IPTG, then cells were grown overnight at either 16°C (top panel) or 24°C (bottom panel). Cells were then harvested and lysed, and samples taken from the insoluble and soluble extracts. Lanes contain: M, molecular weight markers; 1, *E. coli* cell extract before IPTG induction; 2, 4, and 6, soluble cell extracts; 3, 5, and 7, insoluble cell extracts. **d** Coomassie-stained SDS-PAGE gel analysis of the small-scale expression of rHj2a in *E. coli* strain BL21. Lanes contain: M, molecular weight markers; 1, *E. coli* cell extract before IPTG induction; 2, 4, and 6, insoluble cell extracts; 3, 5, and 7, soluble cell extracts.

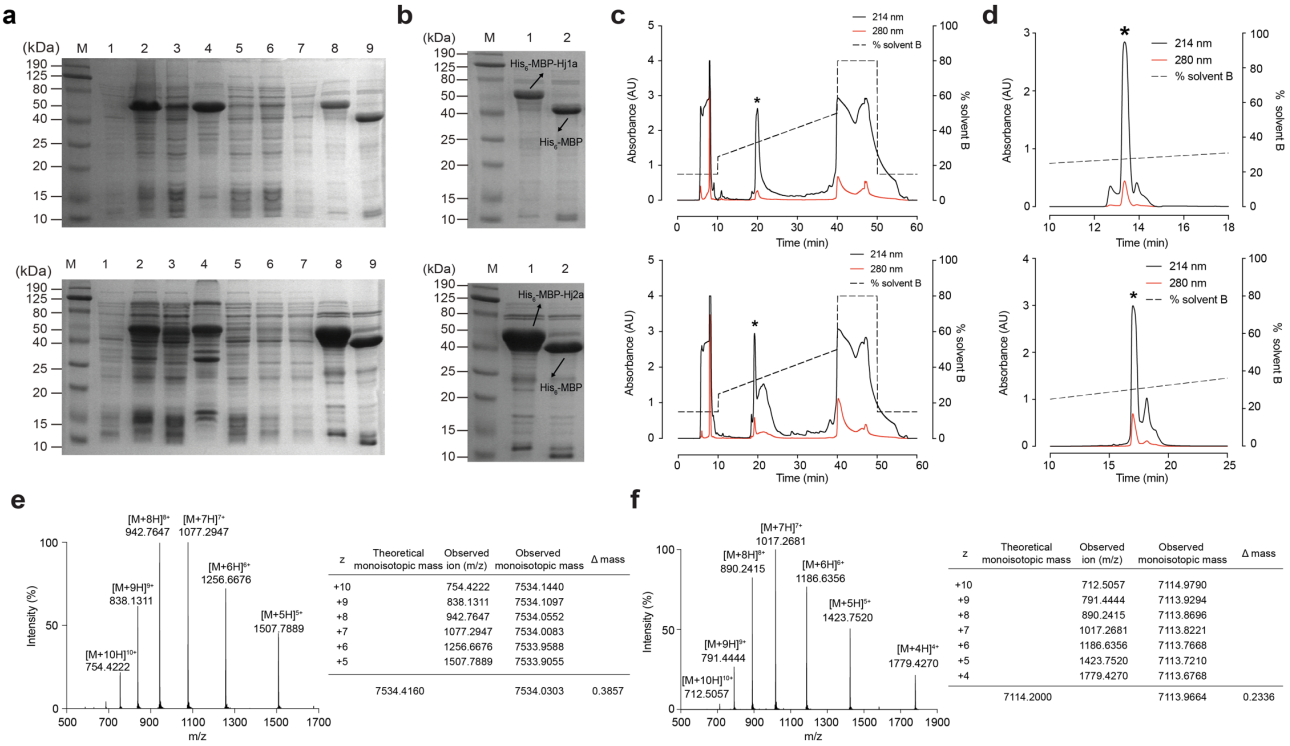

Supplementary Fig. S3 Recombinant expression and purification of rHj1a and rHj2a. **a** Coomassie-stained SDS-PAGE gel demonstrating different steps in the purification of rHj1a (top panel) and rHj2a (bottom panel). Lanes contain: M, molecular weight markers; 1, *E. coli* cell extract before IPTG induction; 2, *E. coli* cell extract after IPTG induction; 3, insoluble cell extract; 4, soluble cell extract after cell disruption; 5, flow-through from Ni-NTA column; 6, first wash from Ni-NTA resin with 1 M imidazole; 7, second wash from Ni-NTA resin with 15 mM imidazole; 8, eluted fusion protein sample before TEV protease cleavage; 9, fusion protein sample after TEV protease cleavage, showing almost complete cleavage of the fusion protein. **b** Cleavage of the His_6-MBP-Hj1a (top panel) and His_6-MBP-Hj2a (bottom panel) fusion protein was found to be 100% complete (lane 2). **c** Semi-preparative RP-HPLC purification of rHj1a (top panel) and rHj2a (bottom panel) using a C_4 column (Phenomenex Jupiter, 250 × 10 mm, 10 µm) with a linear gradient of 25–50% solvent B in solvent A over 30 min (flow rate 3 mL/min). Absorbance was monitored at 214 and 280 nm. Asterisk denotes peak corresponding to correctly folded rHj1a. **d** Chromatograms resulting from final purification of rHj1a (top panel) via analytical RP-HPLC using a Promix MP column (SIELC; 250 × 4.6 mm, 5 µm) with a linear gradient of 25–40% solvent B in solvent A over 20 min (flow rate 0.8 mL/min), and rHj2a (bottom panel) using a Diphenyl column (Agilent; 150 × 3.0 mm, 3 µm) with a linear gradient of 20–40% solvent B in solvent A over 40 min (flow rate 0.6 mL/min). **e** Mass spectrum of rHj1a showing a monoisotopic mass of 7,534.03 Da. **f** Mass spectrum of rHj2a showing a monoisotopic mass of 7113.97 Da.

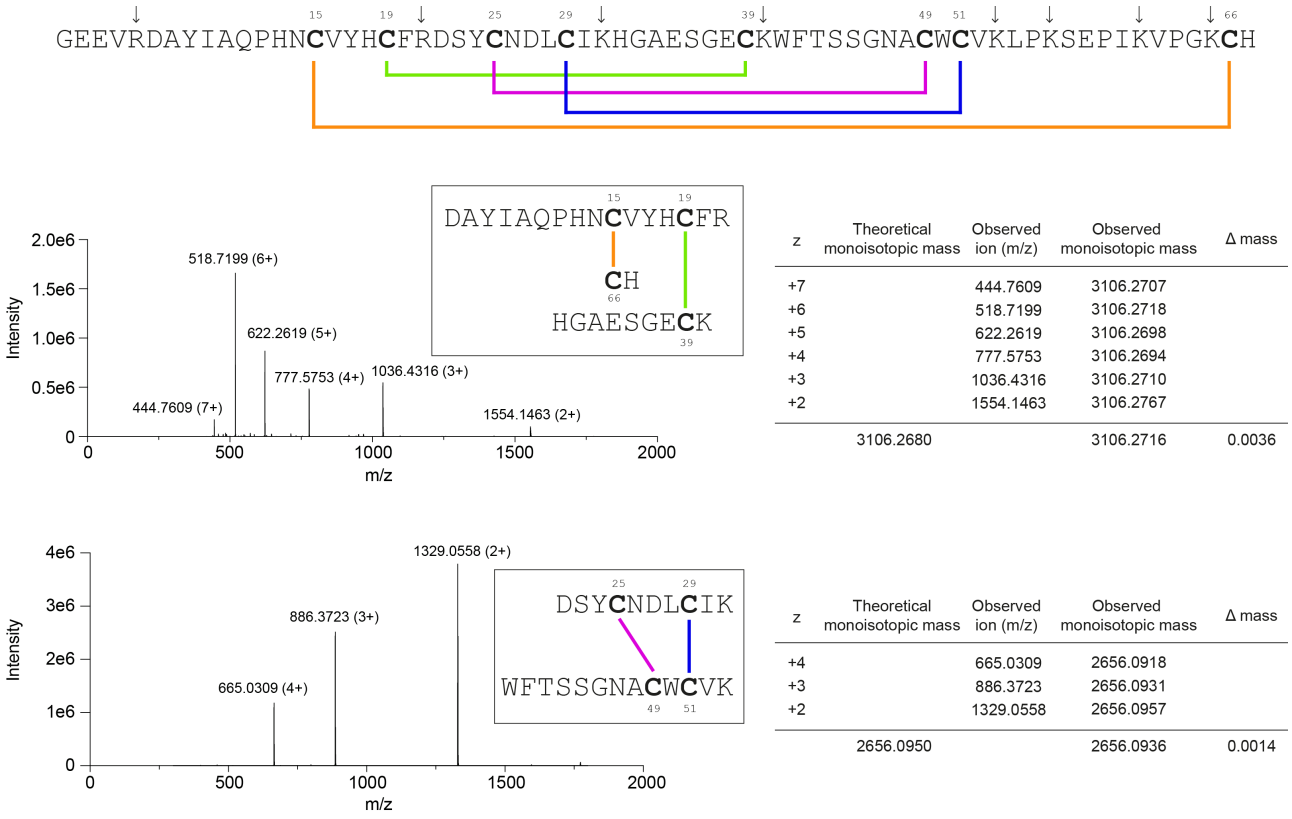

z	Theoretical monoisotopic mass	Observed ion (m/z)	Observed monoisotopic mass	Δ mass
+7		444.7609	3106.2707	
+6		518.7199	3106.2718	
+5		622.2619	3106.2698	
+4		777.5753	3106.2694	
+3		1036.4316	3106.2710	
+2		1554.1463	3106.2767	
	3106.2680		3106.2716	0.0036

z	Theoretical monoisotopic mass	Observed ion (m/z)	Observed monoisotopic mass	Δ mass
+4		665.0309	2656.0918	
+3		886.3723	2656.0931	
+2		1329.0558	2656.0957	
	2656.0950		2656.0936	0.0014

Supplementary Fig. S4. Determination of disulfide linkages in rHj1a. The sequence of Hj1a is shown at top, with cysteine residues in bold and potential tryptic cleavage sites indicated by arrows. Below the sequence are mass spectra of peptide fragments resulting from tryptic digestion of oxidised rHj1a. The peptide digestion fragment (inset) is above the corresponding mass spectrum, along with the theoretical and observed masses in the table on the right. Note that the masses of two fragments are consistent with two predicted peptide digestion products.

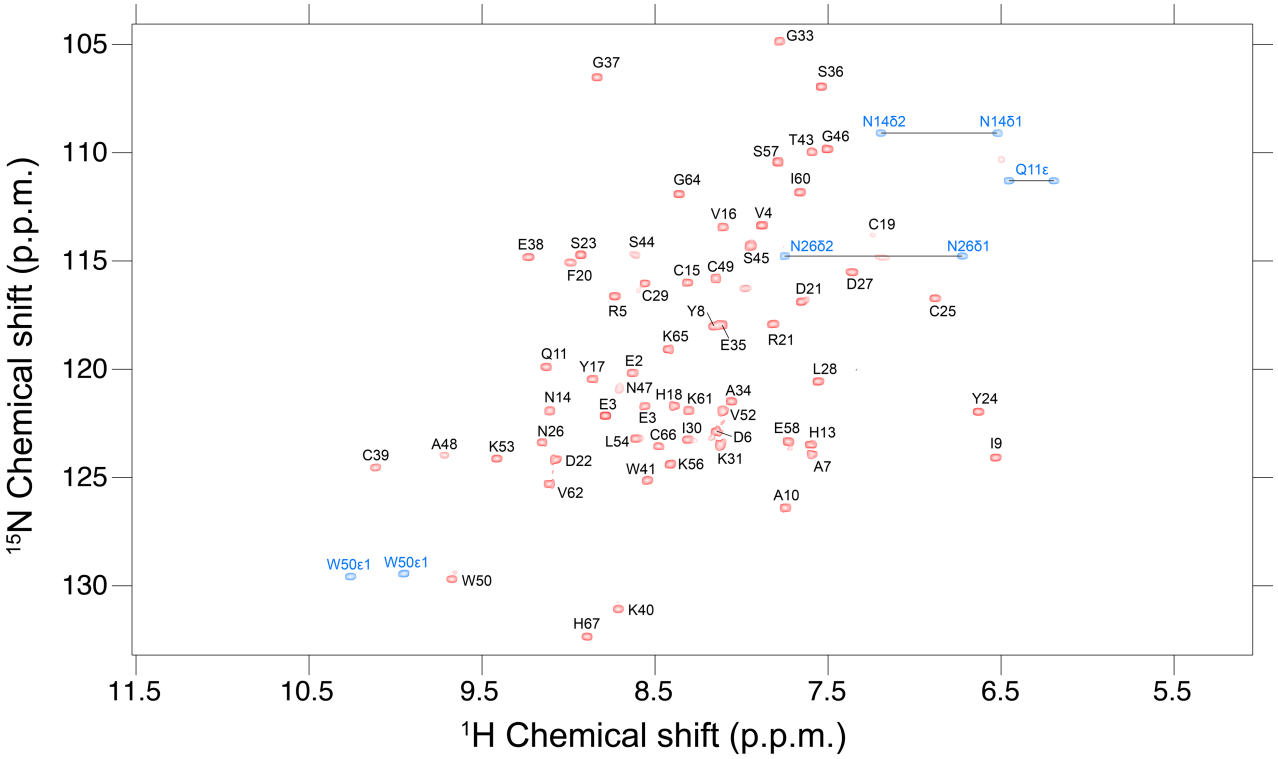

Supplementary Fig. S5 2D ^{1}H–^{15}N HSQC spectrum of ^{13}C/^{15}N-labelled rHj1a showing sequence-specific resonance assignments. The backbone amide nitrogen and proton resonances of rHj1a are well dispersed in the ^{15}N–HSQC NMR spectrum, indicating that rHj1a has a well-ordered tertiary fold. We observed 60 amide protons, including 52 backbone amide peaks plus eight side-chain amide groups of the single Trp residue, single Gln residue, and two Asn residues (i.e., 96.4% of expected peaks assigned, except N-terminal Gly and Pro residues). The broadened resonances of Phe42 could be the result of an intermediate-timescale chemical exchange.

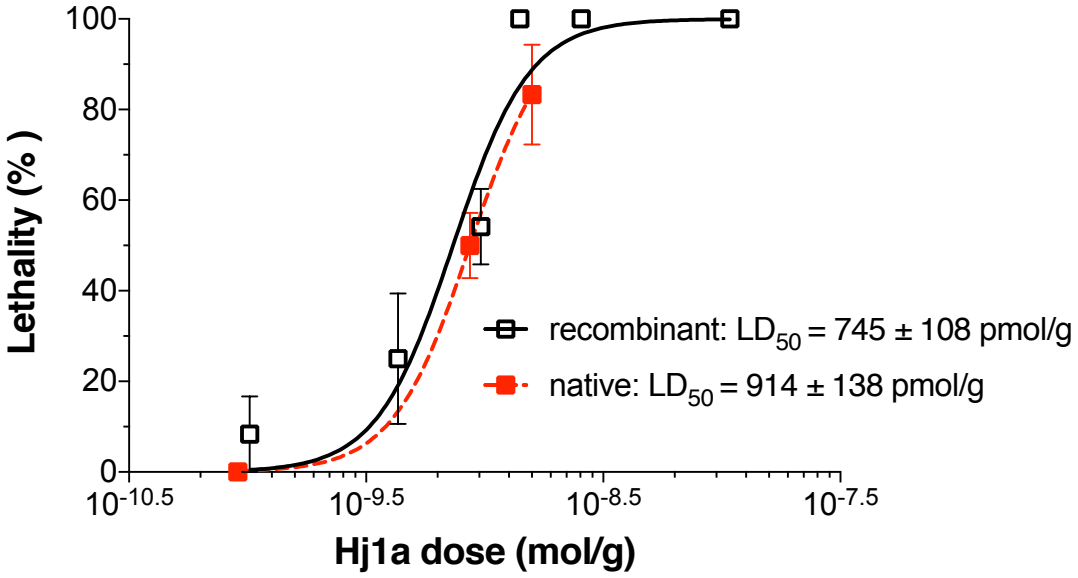

Supplementary Fig. S6 Insecticidal toxicity of Hj1a. Toxin was micro-injected into *Drosophila melanogaster* fruit flies and lethal effects quantified 24 h after injection. No significant difference was observed between the LD_{50} of native and recombinant Hj1a ($p = 0.3903$, Welch's *t*-test).

***L. cuprina* (1.7 µL/fly)**			**15 min**		**30 min**		**1h**		**4h**		**24h**		**48h**		**72h**	
	dose (nmol/g)	*n*	p (%)	d (%)	p (%)	d (%)	p (%)	d (%)	p (%)	d (%)	p (%)	d (%)	p (%)	d (%)	p (%)	d (%)
control	0	8	0	0	0	0	0	0	0	0	0	0	0	0	0	0
Hj1a	4.8	8	0	0	62.5	0	100	0	100	0	87.5	0	87.5	62.5	87.5	87.5
	4.9	8	0	0	75	0	100	0	100	0	87.5	0	100	50	100	75
	4.9	8	0	0	62.5	0	100	0	100	0	87.5	25	75	62.5	75	75
control	0	8	0	0	0	0	0	0	12.5	0	0	0	n.d.	n.d.	n.d.	n.d.
Hj2a	4.8	8	0	0	0	0	0	0	12.5	0	0	0	n.d.	n.d.	n.d.	n.d.
	4.7	8	0	0	0	0	0	0	25	0	0	0	n.d.	n.d.	n.d.	n.d.
	4.9	8	0	0	0	0	0	0	12.5	0	0	0	n.d.	n.d.	n.d.	n.d.

Supplementary Table 1 Insecticidal toxicity for rHj1a and rHj2a injected at a dose of approximately 5 nmol/g at 3 repeats (each $n = 8$) into sheep blowflies (*Lucilia cuprina*) according to previously described procedures [20]. MilliQ water was used as control; the experiment lasted for 72 h post injection; notable toxicity ≥ 50% is highlighted in yellow; p = paralysed (i.e. including all dead flies); d = dead, n.d. = not determined. All flies injected with rHj1a exhibited long-lasting and in most cases irreversible contractile paralysis, setting in about 30 min after injection and lasting for 72 h in some flies. At 15 min after the injection with rHj1a, all flies already showed uncoordinated movement, but not full paralysis. At similar doses, rHj2a did not induce any notable effects in the blowflies within 72 h after the injection.